Histol Histopathol (2015) 30: 1243-1254

http://www.hh.um.es

Histology and Histopathology

Cellular and Molecular Biology

The distribution and time-dependent expression of MAGL during skeletal muscle wound healing in rats

Shu-Kun Jiang, Miao Zhang, Zhi-Ling Tian, Lin-Lin Wang, Rui Zhao, Shan-shan Li, Min Liu, Meng Wang and Da-Wei Guan

Department of Forensic Pathology, China Medical University School of Forensic Medicine, Liaoning Province, P.R. China

Summary. Monoacylglycerol lipase (MAGL) is widely distributed in mammals and largely responsible for metabolizing 2-arachidonoylglycerol (2-AG). Little is known about its expression in skeletal muscles after trauma. A preliminary study on time-dependent expression and distribution of MAGL was performed by immunohistochemical staining, Western blotting and quantitative real-time PCR (qPCR) during skeletal muscle wound healing in rats. An animal model of skeletal muscle contusion was established in 40 Sprague-Dawley male rats. Samples were taken at 1, 3, 5, 7, 9, 13, 17 and 21 days after contusion, respectively (5 rats in each posttraumatic interval). 5 rats were employed as control. Weak immunoreactivity of MAGL was observed in the sarcoplasm of myofibers in control rats. Intensive immunoreactivties of MAGL were observed in polymorphonuclear cells (PMNs), round-shaped mononuclear cells (MNCs), spindle-shaped fibroblastic cells (FBCs) and regenerated multinucleated myotubes in the injured tissue. Subsequently, neutrophils, macrophages and myofibroblasts were identified as MAGL-positive cells by double immunofluorescent procedure. MAGL expression was remarkably up-regulated after contusion by qPCR and Western blot analysis. The results demonstrate that the expression of MAGL is distributed in certain cell types and time-dependently expressed in skeletal muscles after trauma, suggesting that MAGL may be involved in inflammatory response, fibrogenesis and muscle regeneration during skeletal muscle wound healing.

Key words: Skeletal muscle, Trauma, MAGL, Wound repair

Offprint requests to: Da-Wei Guan, M.D., Ph.D., Department of Forensic Pathology, China Medical University School of Forensic Medicine, No.77, Puhe Road, Shenbei New District, Shenyang 110122, Liaoning Province, P. R. China. e-mail: dwguan@aliyun.com, dwguan@mail.cmu.edu.cn

DOI: 10.14670/HH-11-625

Introduction

The endogenous cannabinoid system is composed of the cannabinoid receptor types 1 and 2 (CB1 and CB2 receptor), the endogenous ligands (endocannabinoids) and enzymes that synthesize and degrade endocannabinoids. The two main endocannabinoids, anandamide (AEA) and 2-arachidonoylglycerol (2-AG) are synthesized and released on demand, and metabolized by fatty acid amide hydrolase (FAAH) and monoacylglycerol lipase (MAGL), respectively (Piomelli, 2003). MAGL is a serine hydrolase, originally characterized from the adipose tissue (Labar et al., 2010), where it catalyzes the final step in lipolysis, subsequently releasing free fatty acids and glycerol for fuel or lipid synthesis (Zechner et al., 2012). It has been reported that MAGL is expressed in pre-synaptic nerve terminals of both excitatory and inhibitory neurons in the rodent brains (Dinh et al., 2002; Gulyas et al., 2004).

Skeletal muscle wound healing can be temporally divided into three overlapping phases, the inflammation phase, the regeneration phase and fibrosis phase (Baoge et al., 2012). The process is characterized by necrosis of the damaged myofibers, infiltration of inflammatory

cells, activation of myogenic cells to differentiate and fuse into new myofibers, as well as fibrogenesis initiated by myofibroblasts. During the first phase, the infiltrating inflammatory cells not only phagocytize cellular debris, but also play roles in muscle regeneration and fibrogenesis by releasing a series of cytokines and growth factors (Prisk and Huard, 2003; Zhang et al., 2013). In the endogenous cannabinoid system, MAGL indirectly regulates CB1 and CB2 receptors because MAGL is mainly responsible for hydrolyzing 2-AG, an endogenous ligand for CB1 and CB2 receptors (Sugiura et al., 2006). 2-AG and CB2 receptor play important stimulative roles in oxazolone-induced contact dermatitis in mice (Oka et al., 2006). Activation of the CB1 or CB2 receptor protects against experimental colitis in mice (Storr et al., 2009; Fichna et al., 2014). In addition, 2-AG may act as an anti-fibrogenic mediator in liver by inducing cell death in activated hepatic stellate cells (Siegmund et al., 2007). We have found that MAGL is expressed in neutrophils, macrophages and myofibroblasts during skin-incised wound healing (Ma et al., 2011). All the aforementioned studies suggest that MAGL may be involved in the inflammatory reaction and tissue repair.

Although skeletal muscle wound healing typically is an overlapping event between inflammation and fibrotic repair, the roles of MAGL in this process are not elucidated. The aim of the study is to investigate the time-dependent expression and distribution of MAGL in skeletal muscles after trauma in rats, which is expected to obtain a preliminary insight into the functions of MAGL during skeletal muscle wound healing.

Materials and methods

Animal model of skeletal muscle contusion

A total of 45 healthy, adult Sprague–Dawley male rats, weighing between 290 and 310g, were used. Establishment of the standardized animal model of skeletal muscle contusion in rats has been described previously, which was controllable and reproducible well using a self-designed mechanical weight-drop device (Yu et al., 2010). The instant impact velocity (V) and elastic deformation (DF) at the time of impact are key parameters for impact intensity (Lighthall, 1988). V and DF were monitored and recorded during the experimentation to evaluate the severity of the contusion to muscle. Briefly, 40 rats were anesthetized by intraperitoneal injection with 2% sodium pentobarbital (30 mg/kg) and placed on experimental table in a prone position, and a single impact at velocity of 3 m/s was delivered to the site of the right posterior limb 2.5 cm away from calcaneus with 7.5 mm for DF. The size of impact interface of the counterpoise (weighing 500 g) was 1.127 cm^2. The energy transmitted to the right posterior limb was calculated to be 2.25 J as calculated by the equation: $E=1/2\ mv^2$. After injury, each rat was housed individually and kept under a 12 h light–dark cycle and specific pathogen-free conditions with free access to commercial rat chow and distilled water. All rats were killed by intraperitoneal injection of a lethal dose of pentobarbital (350 mg/kg) at 1, 3, 5, 7, 9, 13, 17 and 21 days after contusion (5 rats at each posttraumatic interval). Muscle sample was taken from the wound site and equally divided into two parts in each rat. One part was used for immunohistochemical procedure, and the other was immediately frozen in liquid nitrogen for Western blotting and quantitative real-time PCR (qPCR), respectively. For the 5 control rats, specimens were collected from the same site after anesthetization with an over-dose of pentobarbital. Experiments complied with the "Principles of Laboratory Animal Care" (National Institutes of Health published no 85-23, revised 1985) that sought to minimize both the number of animals used and any suffering that they might experience and were performed according to the Guidelines for the Care and Use of Laboratory Animals of China Medical University.

Tissue preparation and immunohistochemical staining

The skeletal muscle specimens were immediately fixed in 4% paraformaldehyde in phosphate-buffered saline (PBS) (pH 7.4) for 20 hours. 5 μm-thick paraffin sections were prepared. Immunostaining for MAGL was performed by streptavidin–peroxidase method. After deparaffinization, sections were rehydrated with a series of graded alcohol, and then heated in 0.01 mol/L sodium citrate buffer (pH 6.0) with a medical microwave oven for antigen retrieval. Subsequently, 0.3% H_2O_2-PBS was applied to eliminate endogenous peroxidase. The sections were blocked with 10% non-immune goat serum at room temperature for 1 hour to reduce non-specific reaction. Then, tissue sections were incubated with rabbit anti-MAGL polyclonal antibody (dilution 1:200; ab24701, Abcam, Cambridge, UK) overnight at 4°C, followed by incubation with Histostain-Plus Kit according to the manufacturer's instructions (Zymed Laboratories, South San Francisco, CA, USA). As immunohistochemical controls, some sections were incubated with PBS or normal rabbit IgG in place of the primary antibody. Nuclei were counterstained with hematoxylin. In addition, hematoxylin-eosin (H-E) staining was conventionally conducted.

Cellular localization of MAGL

Detection of MAGL in neutrophils, macrophages or myofibroblasts was conducted by double indirect immunofluorescent procedure. Briefly, deparaffinized sections were blocked with 5% bovine serum albumin (BSA). Then the sections were incubated with rabbit anti-MAGL polyclonal antibody (dilution 1:200; ab24701, Abcam, Cambridge, UK) at room temperature for 2 h. Thereafter, the sections were further incubated with biotinylated donkey anti-rabbit IgG (dilution 1:200; ab6801, Abcam, Cambridge, UK) and streptavidin, Alexa Fluor® 555 conjugate (dilution 1:200; S-21381,

Invitrogen, CA, USA). Then, tissue sections were incubated with mouse anti-myeloperoxidase (MPO) monoclonal antibody (dilution 1:50; sc-271881, Santa Cruz Biotechnology, CA, USA), or anti-Macrophage Marker (MAC387) monoclonal antibody (dilution 1:50; sc-66204, Santa Cruz Biotechnology, CA, USA), or anti-α-smooth muscle actin (α-SMA) monoclonal antibody (dilution 1:200; ab7817, Abcam, Cambridge, UK) overnight at 4°C. After incubation with Alexa Fluor® 488 donkey anti-mouse IgG (dilution 1:200; A21202, Invitrogen, CA, USA) at room temperature for 2 h, the sections were mounted and observed under a fluorescence microscope. Negative controls (sections incubated with normal rabbit or mouse IgG in place of the primary antibodies) were performed concurrently with all staining. The immunofluorescent images were digitally merged.

For positive cell ratio evaluation, 10 microscopic fields were randomly selected at 400-fold magnification in the contused zones in each section, and the ratio of MAGL-positive cells to the total number of cells in each positive cell type was calculated in each microscopic field. The average ratio of the 10 selected microscopic fields was evaluated in each wound specimen and expressed as percentage.

qPCR analysis

Total RNA was isolated from the skeletal muscle specimens with RNAiso Plus (9108, Takara Biotechnology, Shiga, Japan) according to the manufacturer's instructions. OD values of each RNA sample were measured by ultraviolet spectrophotometer. A260/A280 ranged from 1.8 to 2.0. Then, the RNA was reversely transcribed into cDNA using PrimeScript™ RT reagent Kit (RR037A, Takara Biotechnology, Shiga, Japan). The resulting cDNA was used for qPCR with the sequence-specific primer pairs for MAGL and GAPDH (Table 1). The qPCR amplification was performed by Applied Biosystems 7500 Real-Time PCR System (Applied Biosystems, Foster City, CA) using SYBR® PrimeScript™ RT-PCR Kit (RR081A, Takara Biotechnology, Shiga, Japan). Relative amounts of MAGL mRNA was determined using the comparative threshold cycle method (ΔΔCT). Expression of MAGL gene was normalized to the corresponding expression level of GAPDH. The reference gene was chosen based on a set of guidelines that describe the information necessary for evaluating qPCR experiments (Bustin et al., 2009). To exclude any potential contamination, negative controls were also performed with dH2O instead of cDNA during each run. No amplification product was detected. The qPCR procedure was repeated at least three times for each sample.

Protein preparation and immunoblotting assay

The skeletal muscle samples were ground into powder with liquid nitrogen using a grinder and homogenized with a sonicator in RIPA buffer (sc-24948, Santa Cruz Biotechnology, CA, USA) containing protease inhibitors at 4°C. Homogenates were centrifuged at 12,000xg for 10 min at 4°C three times, and the resulting supernatants were collected. The protein concentrations were determined using bicinchoninic acid method. Aliquots of the supernatants were diluted in an equal volume of 6x electrophoresis sample buffer and boiled for 5 min. Protein lysates (30 μg) were separated on a 12% sodium dodecyl sulfate-poly-acrylamide electrophoresis gel and transferred onto polyvinylidene fluoride membranes (Millipore, Billerica, MA, USA). After being blocked with 5% BSA in Tris-buffered saline-Tween#20 at room temperature for 2 h, the blots were incubated with rabbit anti-MAGL polyclonal antibody (dilution 1:200; ab24701, Abcam, Cambridge, UK) at 4°C overnight and horseradish peroxidase conjugated goat anti-rabbit IgG (sc-2004, Santa Cruz Biotechnology, CA, USA) at 1:2,000 dilution at room temperature for 2 h. The blotting was visualized with Western blotting luminol reagent (sc-2048, SantaCruz Biotechnology, CA, USA) by Electrophoresis Gel Imaging Analysis System (MF-ChemiBIS 3.2, DNR Bio-Imaging Systems, ISR). Subsequently, densitometric analyses of the bands were semi-quantitatively conducted using Scion Image Software (Scion Corporation, MD, USA). The relative protein levels were calculated by comparison with the amount of GAPDH (#G13-61M, SignalChem, Canada) as a loading control.

Statistical analysis

Data were expressed as mean ± standard deviation (SD) and analyzed using SPSS for Windows 13.0. Parametric data were analyzed by one-way ANOVA between two groups. Non-parametric data were analyzed

Table 1. qPCR primer sequences.

Gene	Species		Position	Product size (bp)
MAGL	Rodent	Forward:5'- CCAACTCTGTCCTCCATGAAATA -3' Reverse:5'-GGTTCCCTAGACAGCACATTC-3'	953-976 1028-1049	96
GAPDH	Rodent	Forward:5'-CATCTCCCTCACAATTCCATCC-3'x Reverse:5'-GAGGGTGCAGCGAACTTTAT-3	1177-1199 1257-1277	100

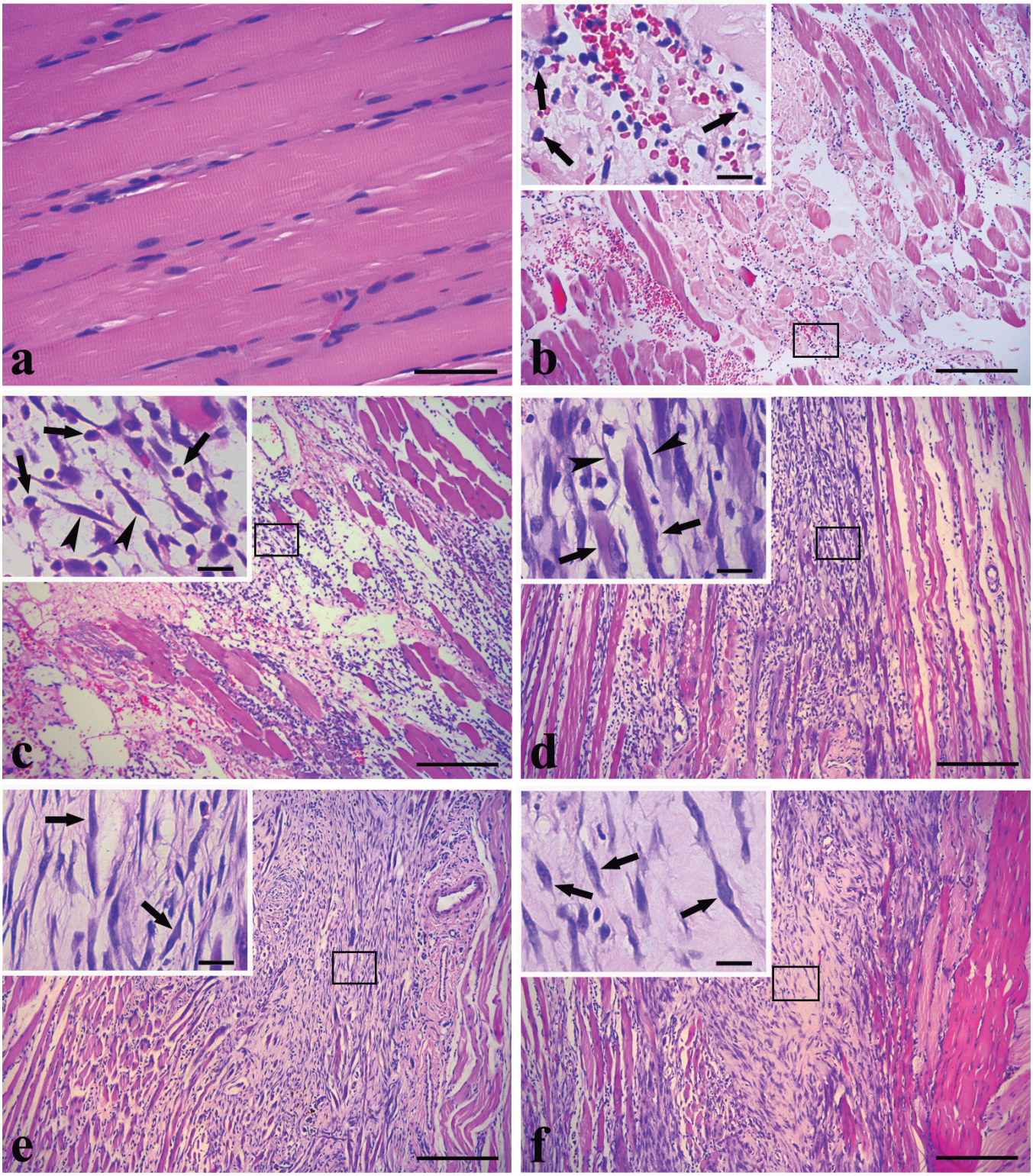

Fig. 1. H-E staining in rat skeletal muscle contusion. **a.** The morphology of normal skeletal muscles as a control. **b.** Polymorphonuclear cells (PMNs) are detected at 1 day after contusion (arrows). **c.** Round-shaped mononuclear cells (MNCs, arrows) and spindle-shaped fibroblastic cells (FBCs, arrowheads) are present in the injured tissue at 3 days after contusion. **d.** FBCs (arrowheads), concomitant with regenerated multinucleated myotubes (arrows) are observed in the areas of contusion at 5 days after contusion. **e, f.** Spindle-shaped FBCs (arrows) and fibrotic tissue are still seen in the wound zone from 13 days to 21 days after contusion. Scale bar: A, 50 μm; B-F, 200 μm; insets, 10 μm.

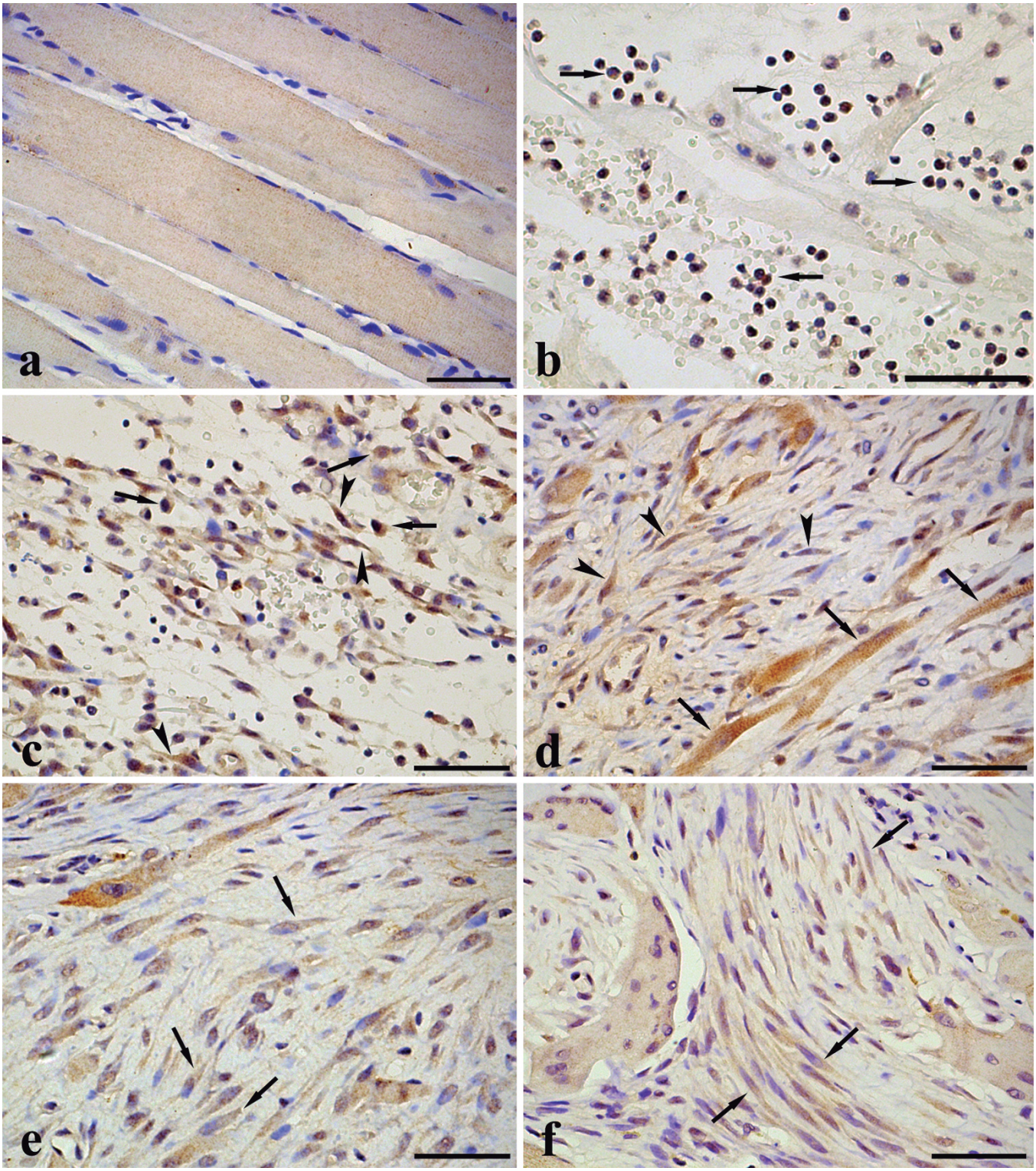

Fig. 2. Immunohistochemical staining of MAGL in rat skeletal muscle contusion. **a.** MAGL immunoreactivity is seen in sarcoplasm of skeletal muscles. **b.** MAGL-positive staining is observed in PMNs (arrows) at 1 day after contusion. **c.** MAGL-positive staining is observed in MNCs (arrows) and FBCs (arrowheads) at 3 days after contusion. **d.** MAGL-positive staining is observed in FBCs (arrowheads) and regenerated multinucleated myotubes (arrows) at 5 days after contusion. **e, f.** At 13 and 21 days after contusion, there are a large number of FBCs (arrows) labeled with anti-MAGL antibody in the wound zones. Scale bar: 50 μm

by a Mann Whitney U test between two groups. Difference associated with $P<0.05$ was considered as statistic significance.

Results

Histological examination

In sections stained with H-E, hemorrhage, edema and degeneration were observed in the contused skeletal muscles. A great number of polymorphonuclear cells (PMNs) appeared in wound zones at 1 day post-wounding (Fig. 1b). Round-shaped mononuclear cells (MNCs) appeared in wound zones at 1 day, which remarkably increased in number at 3 day post-wounding. At 3 days post-wounding, spindle-shaped fibroblastic cells (FBCs) appeared in the wound zones (Fig. 1c). From 5 to 9 days post-wounding, a large number of FBCs, concomitant with regenerated multinucleated myotubes were observed in the wounds (Fig. 1d). From 13 to 21 days post-wounding, FBCs and fibrotic tissue were still observed in the wounds (Fig. 1e, f).

Immunohistochemical and double indirect immunofluorescence analyses

In the control skeletal muscle specimens, a weak positive immunoreactivity for MAGL was detected in sarcoplasm of rat skeletal muscle fibers (Fig. 2a). In the injured skeletal muscle samples, most PMNs showed MAGL-positive at 1 day post-wounding (Fig. 2b). At 3 days post-wounding, a great number of MNCs and FBCs

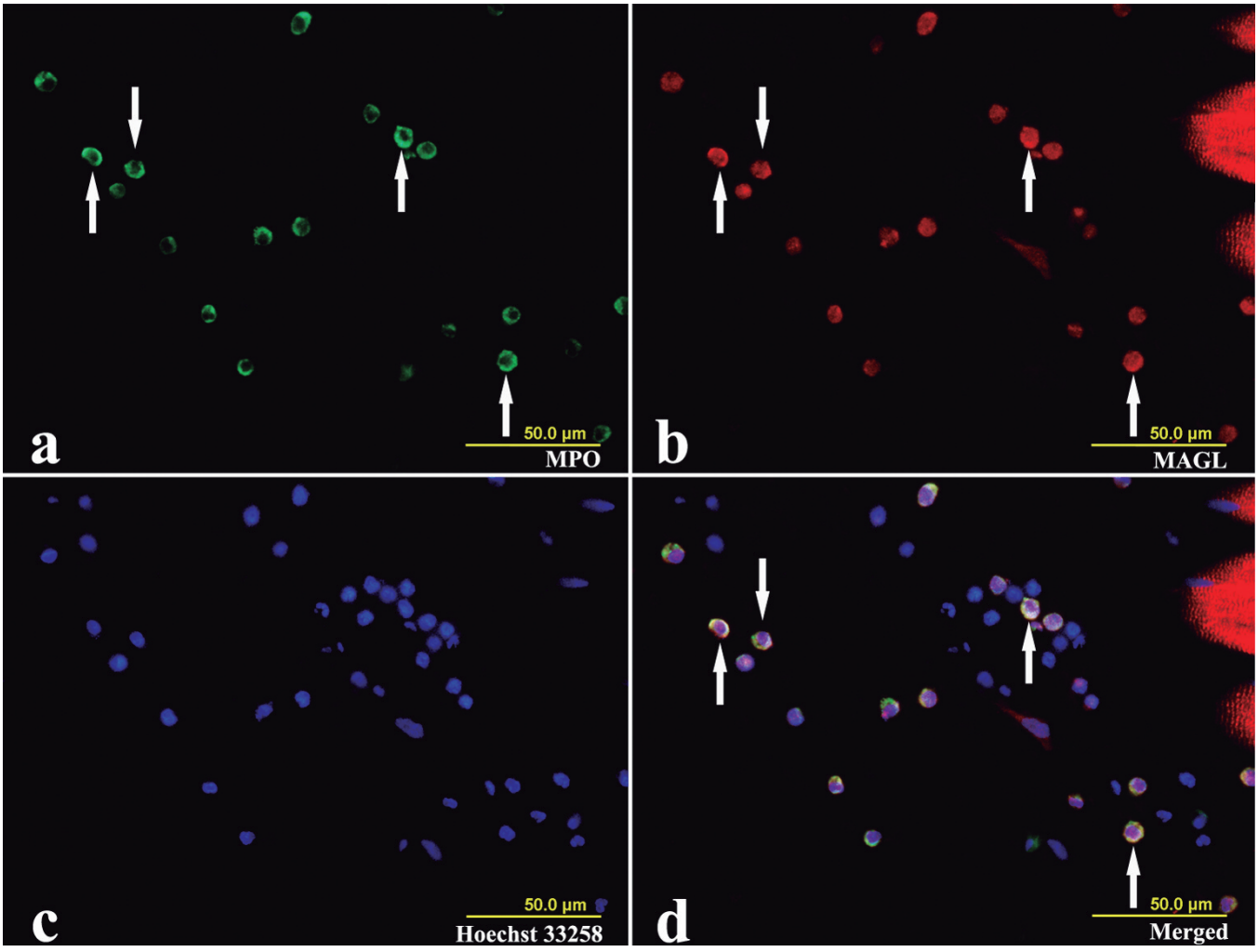

Fig. 3. Double immunofluorescent staining was performed for identifying MAGL-expressing neutrophils at 1 day after contusion. **a.** The sample was immunostained with anti-MPO (green). **b.** The sample was immunostained with anti-MAGL (red). **c.** Nuclei were counterstained with Hoechst 33258 (blue). **d.** Signals in **a-c** were digitally merged. The $MAGL^+/MPO^+$ cells are presented as yellow signal in the merged image. Representative results from at least three individual experiments are shown. Scale bar: 50 μm.

were positively immunostained with anti-MAGL antibody (Fig. 2c). From 5 to 9 days post-wounding, MAGL immunoreactivity was mainly detected in FBCs and regenerated multinucleated myotubes (Fig. 2d). From 13 to 21 days post-wounding, there were still FBCs labeled with anti-MAGL antibody in the fibrotic tissue (Fig. 2e,f).

For the identification of PMNs, MNCs and FBCs, co-localization of MAGL and MPO (neutrophil marker), or MAGL and MAC387 (macrophage marker) , or MAGL and α-SMA (myofibroblast marker) were conducted. In the control skeletal muscle specimens, no $MAGL^+/MPO^+$ cells were observed, but a few $MAGL^+/MAC387^+$ cells were detected in the perimysium and epimysium of normal skeletal muscle. At 1 day post-wounding, a great number of PMNs infiltrated into the injured sites showed $MAGL^+/MPO^+$ (Fig. 3). After 1 day post-injury, the double-positive cells decreased in number at the wound zones. At 3 days post-wounding, a large number of MNCs infiltrated into the injured sites showed $MAGL^+/MAC387^+$ (Fig. 4). From 5 days post-wounding, fewer double-positive cells were detected in the wound zones. With extension of posttraumatic interval, a large number of $MAGL^+/\alpha$-SMA^+ cells were observed (Fig. 5). After 7 days post-wounding, $MAGL^+/\alpha$-SMA^+ cells decreased in number gradually. In negative controls, little green fluorescence was seen and weak auto-fluorescence was observed in myofibers (Fig. 6).

The average ratios of $MAGL^+$ neutrophils, macrophages, and myofibroblasts were evaluated. Gradual reductions in the average ratios of $MAGL^+$ neutrophils were detected at 1, 3 and 5 days post-wounding. The average ratios of $MAGL^+$ macrophages

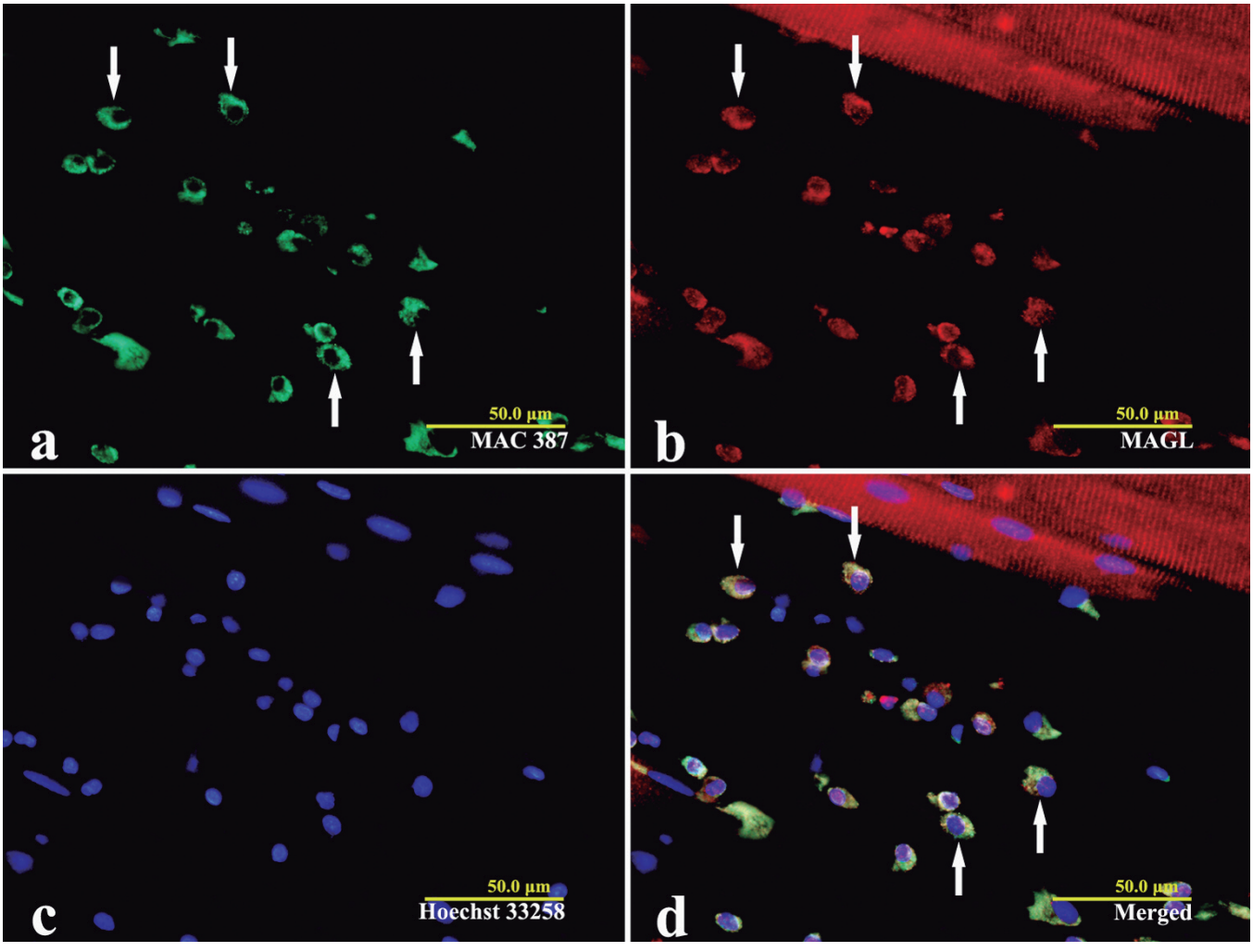

Fig. 4. Double immunofluorescent staining was performed for identifying MAGL-expressing macrophages at 3 days after contusion. **a.** The sample was immunostained with anti-MAC387 (green). **b.** The sample was immunostained with anti-MAGL (red). **c.** Nuclei were counterstained with Hoechst 33258 (blue). **d.** Signals in **a-c** were digitally merged. The $MAGL^+/MAC387^+$ cells are presented as yellow signal in the merged image. Representative results from at least three individual experiments are shown. Scale bar: 50 μm.

and myofibroblasts maximized at 5 and 7 days post-wounding, respectively. In each positive cell type, there was a significant difference between two adjacent posttraumatic intervals (Fig. 7).

qPCR and Western blotting

Relative quantity of MAGL mRNA expression in rat skeletal muscle was assayed by qPCR throughout the 21 days after contusion. The MAGL mRNA expression was generally up-regulated within 7 days post-wounding and down-regulated thereafter. There were significant differences between control group and 3 and 7 days post-wounding in the expression of MAGL mRNA (Fig. 8).

The expression of MAGL protein can be detected in all skeletal muscle specimens including the control by Western blotting. A significant increase in the relative protein level of MAGL to GAPDH was found at 5, 7, 9 and 13 days post-wounding as compared with that of control, which maximized at 9 days by semi-quantitative analysis. There were significant differences in the relative intensity of MAGL to GAPDH between 5, 7, 13 or 17 days injury groups and their preceding groups (Fig. 9a,b).

Discussion

Damage to skeletal muscle caused by blunt trauma presents pathologically a typical inflammatory process during repair. The early phase of muscle injury is accompanied by inflammatory cells infiltration in the damaged muscles. Neutrophils firstly invade into the

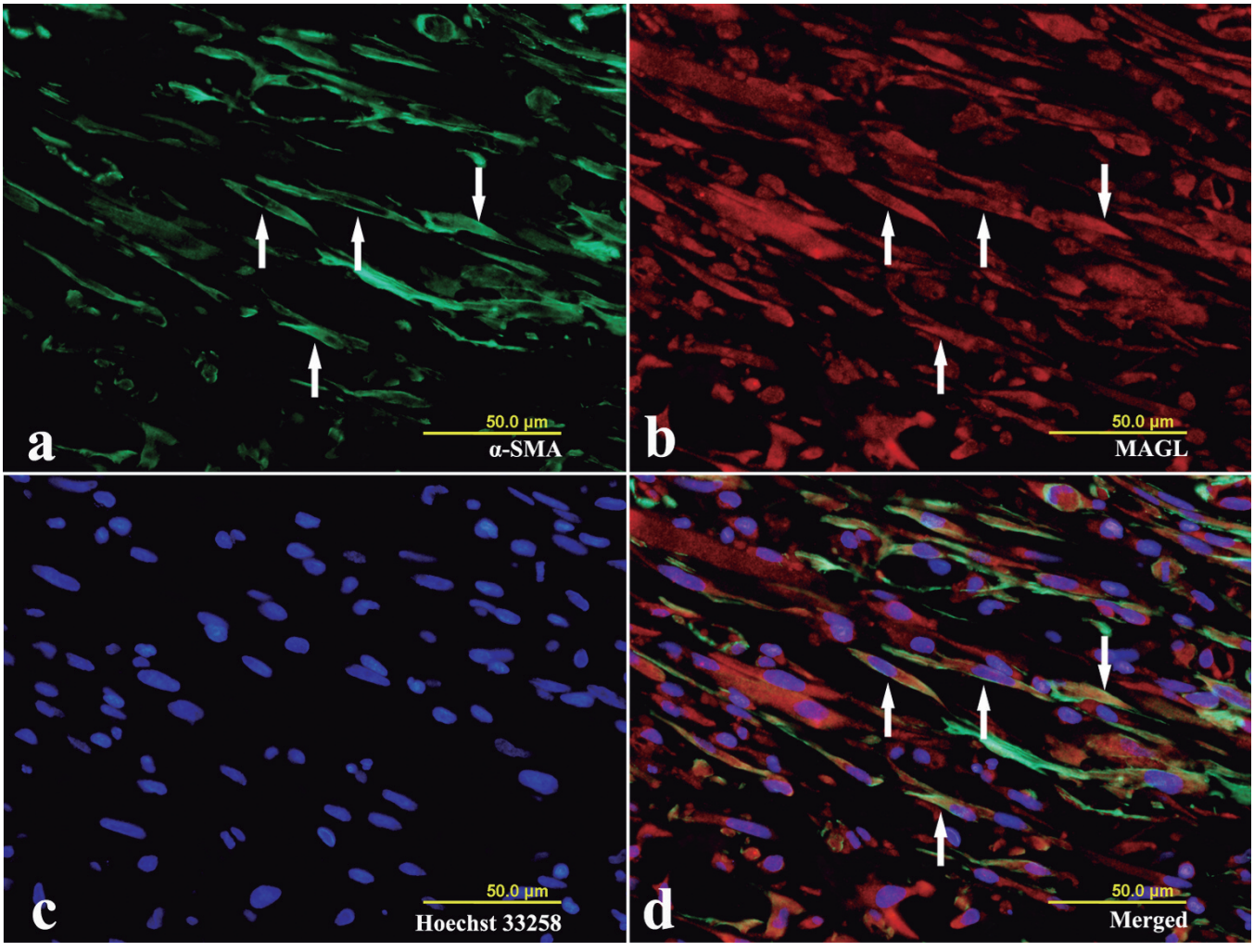

Fig. 5. Double immunofluorescent staining was performed for identifying MAGL-expressing myofibroblasts at 7 days after contusion. **a.** The sample was immunostained with anti-α-SMA (green). **b.** The sample was immunostained with anti-MAGL (red). **c.** Nuclei were counterstained with Hoechst 33258 (blue). **d.** Signals in **a-c** were digitally merged. The MAGL$^+$/α-SMA$^+$ cells are presented as yellow signal in the merged image. Representative results from at least three individual experiments are shown. Scale bar: 50 μm.

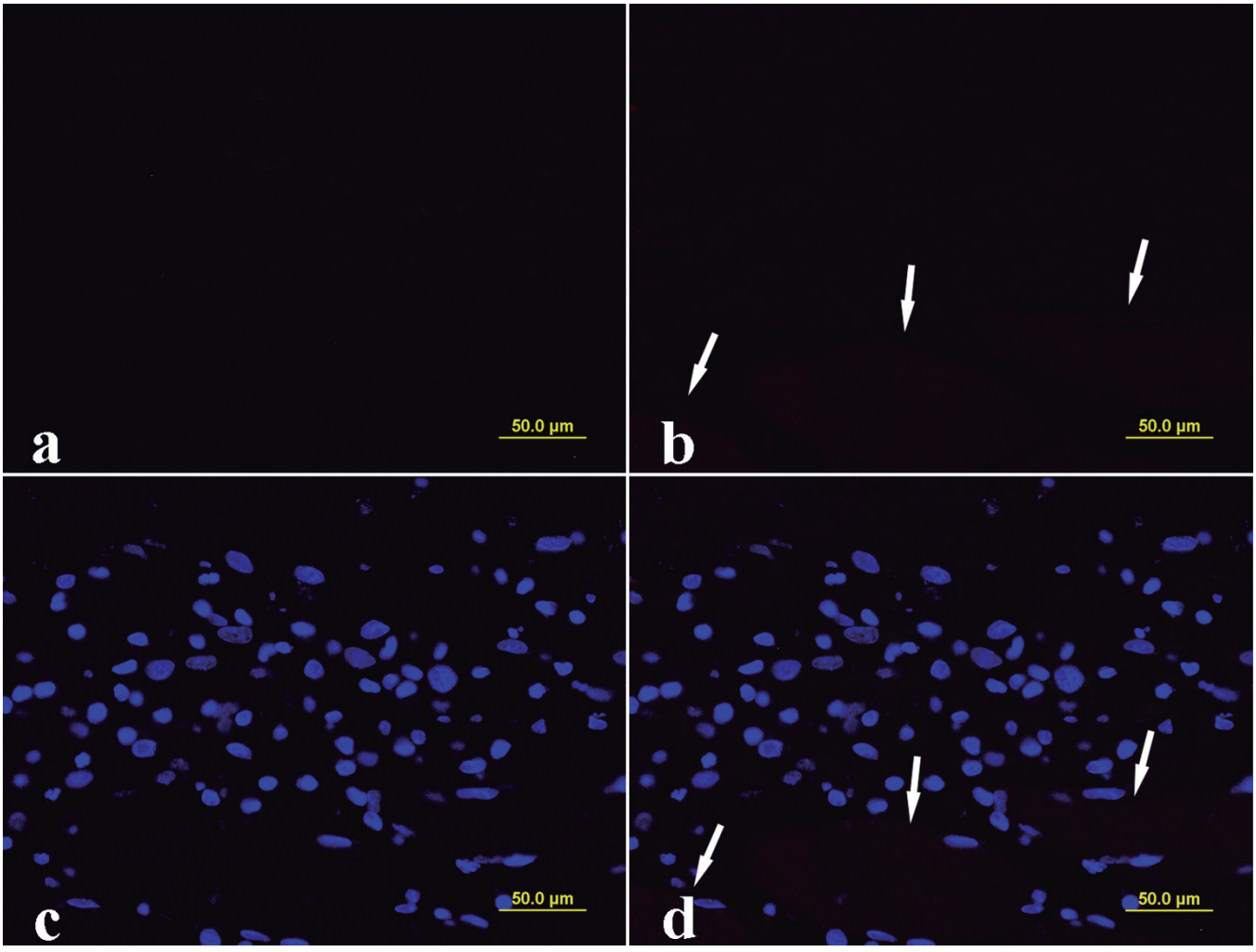

Fig. 6. Negative controls. **a.** Little green auto-fluorescence is observed. **b**. Myofibers show weak red auto-fluorescence (arrows). **c.** Nuclei were counterstained with Hoechst 33258 (blue). **d.** Signals in **a-c** were digitally merged. Representative results from at least three individual experiments are shown. Scale bar: 50 μm.

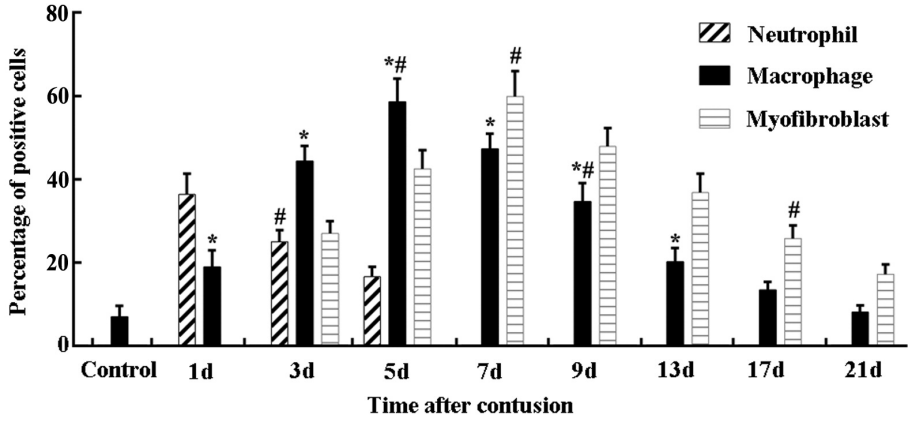

Fig. 7. The average ratios of MAGL-positive neutrophils, macrophages and myofibroblasts in relation to wound age. The average ratios of MAGL-positive neutrophils, macrophages and myofibroblasts peaked at 1, 5 and 7 days post-wounding, respectively. Data were presented as mean ± SD and analyzed using one-way ANOVA. *: P<0.05 (vs control group), #: P < 0.05 (vs preceding posttraumatic group).

injured tissues. Subsequently, macrophages are predominant at injured site, which phagocytose cellular debris and remove the disrupted tissues (Karalaki et al., 2009). Our present study confirmed the similar findings on morphological changes.

MAGL releases arachidonic acid for the synthesis of

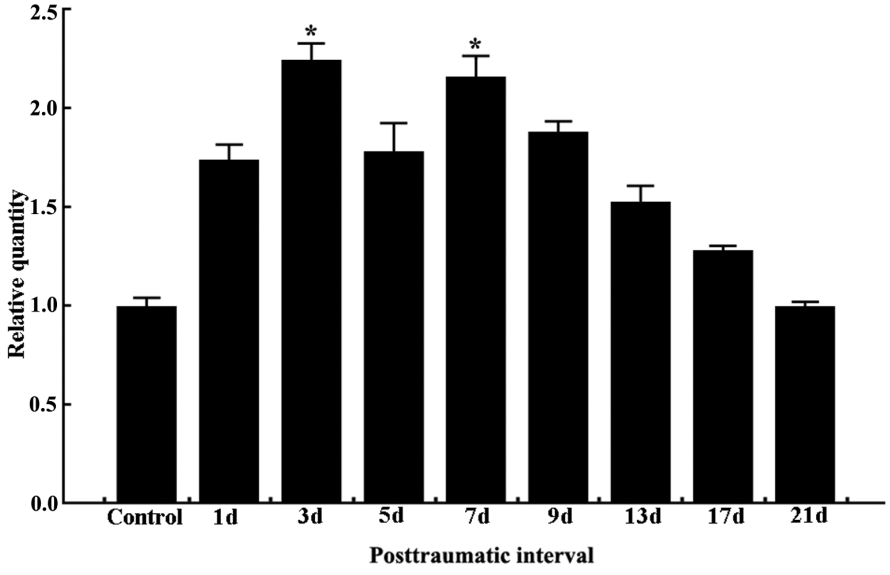

Fig. 8. Analysis of MAGL and GAPDH mRNA expression from skeletal muscle specimens by real-time PCR. Relative quantity of MAGL mRNA was normalized to the expression level of GAPDH. Significant increases in the relative quantity of MAGL mRNA expression were observed at 3 and 7 days post-wounding as compared with that of control. Data were presented as mean ± SD (n=5) and analyzed using Mann Whitney U test. *: P<0.05 (vs control group).

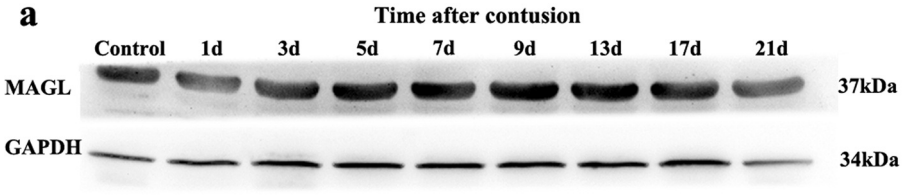

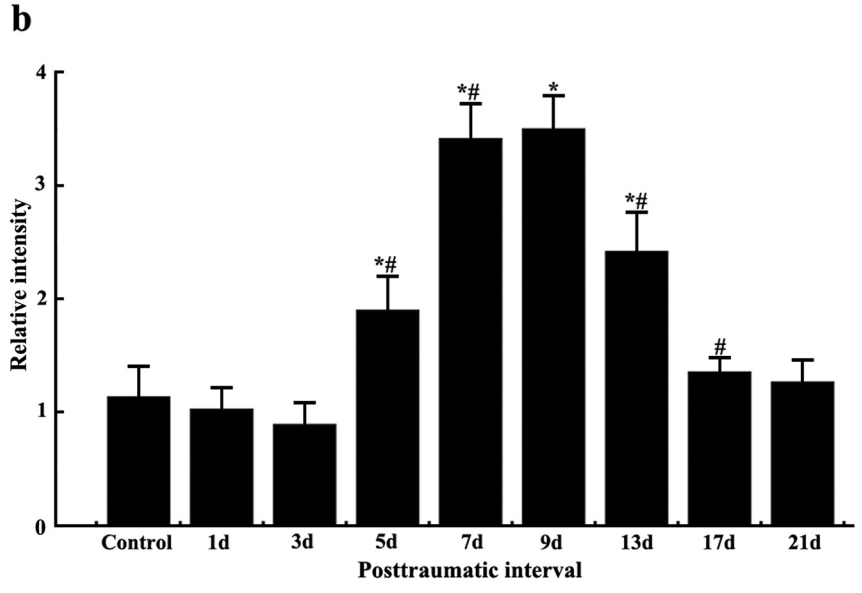

Fig. 9. a. Analysis of MAGL and GAPDH protein from skeletal muscle specimens by Western blotting. Representative results from five individual animals are shown. **b.** Relative intensity of MAGL to GAPDH. Significant increases in the relative protein levels of MAGL to GAPDH were observed at 5, 7, 9 and 13 days post-wounding as compared with that of control. Data were presented as mean ± SD (n=5) and analyzed using one-way ANOVA. *: P<0.05 (vs control group), #: P<0.05 (vs preceding post-traumatic group).

pro-inflammatory eicosanoids in certain tissues such as the brain, liver, and lung (Nomura et al., 2011). Inhibition of MAGL alleviates the inflammatory response in colitis and acute lung injury (Alhouayek et al., 2011; Costola-de-Souza et al., 2013), and suppresses inflammatory nociception in a carrageenan-induced paw edema and mechanical allodynia model (Ghosh et al., 2013). These observations suggest an involvement of MAGL in inflammatory response. In the present study, we observed that MAGL was expressed in neutrophils and macrophages, and the average ratios of MAGL-positive neutrophils and macrophages reached peaks at inflammatory phase after contusion. In addition, the expression of MAGL was up-regulated at protein and gene levels at inflammatory phase in skeletal muscles after trauma. Therefore, we speculate that MAGL may be involved in response to inflammation during skeletal muscle wound healing. Furthermore, a study on the stimulus-induced biosynthesis and inactivation of 2-AG in circulating and tumoral macrophages demonstrated that macrophages participate in the homeostasis of 2-AG through metabolic mechanisms, including the hydrolysis of MAGL and FAAH (Di Marzo et al., 1999). Therefore, it is assumed that MAGL expressed by macrophages may play a role in the maintenance of 2-AG level during the skeletal muscle wound healing in rats.

Hitherto, there have been no reports on the roles of MAGL in fibrogenesis. As previously reported, MAGL indirectly regulates CB1 and CB2 receptors in the endogenous cannabinoid system (Sugiura et al., 2006). It has been demonstrated that CB1 and CB2 receptors are closely involved in hepatic cirrhosis produced by hepatic myofibroblasts. Endogenous activation of CB2 receptor exhibits anti-fibrosis action which is opposite to stimulation of CB1 receptor (Julien et al., 2005; Teixeira-Clerc et al., 2006). Myofibroblasts, which are characterized by a contractile phenotype and the presence of α-SMA stress fibers, play an important role in collagen synthesis and fibrosis (Lotersztajn et al., 2005). Our previous study showed that CB2 receptor was detected in FBCs during skeletal muscle wound healing (Yu et al., 2010). In the present study, immunostaining for MAGL was also observed in FBCs, and these MAGL-positive FBCs were identified as myofibroblasts. Furthermore, the protein level of MAGL peaked at initial stage of fibrogenesis after contusion when a large number of MAGL-positive myofibroblasts were observed. It is presumed that MAGL may play a role in modulating the fibrotic repair during the skeletal muscle wound healing.

Muscle regeneration is a critical event for functional recovery of injured skeletal muscles (Filippin et al., 2011). In the regeneration stage, the activated satellite cells proliferate and differentiate into myoblasts. The newly formed myoblasts fuse with each other to form multinucleated myofibers (Jarvinen et al., 2005). In the inflammation phase, macrophages are essential for the triggering of muscle regeneration following by activating quiescent satellite cells (Lescaudron et al., 1999). Apart from macrophages, regenerated multinucleated myotubes was showed to express MAGL in our present study. We presumed that MAGL may also be involved in modulating skeletal muscle regeneration.

In conclusion, we demonstrate that MAGL is distributed in neutrophils, macrophages, myofibroblasts and regenerated multinucleated myotubes and time-dependently expressed, suggesting that MAGL may be involved in inflammatory response, fibrogenesis and muscle regeneration during skeletal muscle wound healing.

Acknowledgements. The study was financially supported in part by grants from research fund for the Doctoral Program funded by Ministry of Education of China (20122104110025) and from projects funded by National Natural Science Foundation of China (81273342) and Shenyang Science and Technology Bureau (F12-277-1-03)

References

Alhouayek M., Lambert D.M., Delzenne N.M., Cani P.D. and Muccioli G.G. (2011). Increasing endogenous 2-arachidonoylglycerol levels counteracts colitis and related systemic inflammation. FASEB J. 25, 2711-2721.

Baoge L., Van Den Steen E., Rimbaut S., Philips N., Witvrouw E., Almqvist K.F., Vanderstraeten G. and Vanden Bossche L.C. (2012). Treatment of skeletal muscle injury: A review. ISRN Orthop. 2012, 689012.

Bustin S.A., Benes V., Garson J.A., Hellemans J., Huggett J., Kubista M., Mueller R., Nolan T., Pfaffl M.W., Shipley G.L., Vandesompele J. and Wittwer C.T. (2009). The miqe guidelines: Minimum information for publication of quantitative real-time pcr experiments. Clin. Chem. 55, 611-622.

Costola-de-Souza C., Ribeiro A., Ferraz-de-Paula V., Calefi A.S., Aloia T.P., Gimenes-Junior J.A., de Almeida V.I., Pinheiro M.L. and Palermo-Neto J. (2013). Monoacylglycerol lipase (magl) inhibition attenuates acute lung injury in mice. PLoS One 8, e77706.

Di Marzo V., Bisogno T., De Petrocellis L., Melck D., Orlando P., Wagner J.A. and Kunos G. (1999). Biosynthesis and inactivation of the endocannabinoid 2-arachidonoylglycerol in circulating and tumoral macrophages. Eur. J. Biochem. 264, 258-267.

Dinh T.P., Carpenter D., Leslie F.M., Freund T.F., Katona I., Sensi S.L., Kathuria S. and Piomelli D. (2002). Brain monoglyceride lipase participating in endocannabinoid inactivation. Proc. Natl. Acad. Sci. USA 99, 10819-10824.

Fichna J., Bawa M., Thakur G.A., Tichkule R., Makriyannis A., McCafferty D.M., Sharkey K.A. and Storr M. (2014). Cannabinoids alleviate experimentally induced intestinal inflammation by acting at central and peripheral receptors. PLoS One 9, e109115.

Filippin L.I., Cuevas M.J., Lima E., Marroni N.P., Gonzalez-Gallego J. and Xavier R.M. (2011). Nitric oxide regulates the repair of injured skeletal muscle. Nitric Oxide 24, 43-49.

Ghosh S., Wise L.E., Chen Y., Gujjar R., Mahadevan A., Cravatt B.F. and Lichtman A.H. (2013). The monoacylglycerol lipase inhibitor jzl184 suppresses inflammatory pain in the mouse carrageenan model. Life Sci. 92, 498-505.

Gulyas A.I., Cravatt B.F., Bracey M.H., Dinh T.P., Piomelli D., Boscia F. and Freund T.F. (2004). Segregation of two endocannabinoid-

hydrolyzing enzymes into pre- and postsynaptic compartments in the rat hippocampus, cerebellum and amygdala. Eur. J. Neurosci. 20, 441-458.

Jarvinen T.A., Jarvinen T.L., Kaariainen M., Kalimo H. and Jarvinen M. (2005). Muscle injuries: Biology and treatment. Am. J. Sports Med. 33, 745-764.

Julien B., Grenard P., Teixeira-Clerc F., Van Nhieu J.T., Li L., Karsak M., Zimmer A., Mallat A. and Lotersztajn S. (2005). Antifibrogenic role of the cannabinoid receptor cb2 in the liver. Gastroenterology 128, 742-755.

Karalaki M., Fili S., Philippou A. and Koutsilieris M. (2009). Muscle regeneration: Cellular and molecular events. In Vivo 23, 779-796.

Labar G., Wouters J. and Lambert D.M. (2010). A review on the monoacylglycerol lipase: At the interface between fat and endocannabinoid signalling. Curr. Med. Chem. 17, 2588-2607.

Lescaudron L., Peltekian E., Fontaine-Perus J., Paulin D., Zampieri M., Garcia L. and Parrish E. (1999). Blood borne macrophages are essential for the triggering of muscle regeneration following muscle transplant. Neuromuscul. Disord. 9, 72-80.

Lighthall J.W. (1988). Controlled cortical impact: A new experimental brain injury model. J. Neurotrauma. 5, 1-15.

Lotersztajn S., Julien B., Teixeira-Clerc F., Grenard P. and Mallat A. (2005). Hepatic fibrosis: Molecular mechanisms and drug targets. Annu. Rev. Pharmacol. Toxicol. 45, 605-628.

Ma W.X., Yu T.S., Fan Y.Y., Zhang S.T., Ren P., Wang S.B., Zhao R., Pi J.B. and Guan D.W. (2011). Time-dependent expression and distribution of monoacylglycerol lipase during the skin-incised wound healing in mice. Int J Legal Med 125, 549-558.

Nomura D.K., Morrison B.E., Blankman J.L., Long J.Z., Kinsey S.G., Marcondes M.C., Ward A.M., Hahn Y.K., Lichtman A.H., Conti B. and Cravatt B.F. (2011). Endocannabinoid hydrolysis generates brain prostaglandins that promote neuroinflammation. Science 334, 809-813.

Oka S., Wakui J., Ikeda S., Yanagimoto S., Kishimoto S., Gokoh M., Nasui M. and Sugiura T. (2006). Involvement of the cannabinoid cb2 receptor and its endogenous ligand 2-arachidonoylglycerol in oxazolone-induced contact dermatitis in mice. J. Immunol. 177, 8796-8805.

Piomelli D. (2003). The molecular logic of endocannabinoid signalling. Nat. Rev. Neurosci. 4, 873-884.

Prisk V. and Huard J. (2003). Muscle injuries and repair: The role of prostaglandins and inflammation. Histol. Histopathol. 18, 1243-1256.

Siegmund S.V., Qian T., de Minicis S., Harvey-White J., Kunos G., Vinod K.Y., Hungund B. and Schwabe R.F. (2007). The endocannabinoid 2-arachidonoyl glycerol induces death of hepatic stellate cells via mitochondrial reactive oxygen species. FASEB J. 21, 2798-2806.

Storr M.A., Keenan C.M., Zhang H., Patel K.D., Makriyannis A. and Sharkey K.A. (2009). Activation of the cannabinoid 2 receptor (cb2) protects against experimental colitis. Inflamm. Bowel. Dis. 15, 1678-1685.

Sugiura T., Kishimoto S., Oka S. and Gokoh M. (2006). Biochemistry, pharmacology and physiology of 2-arachidonoylglycerol, an endogenous cannabinoid receptor ligand. Prog. Lipid. Res. 45, 405-446.

Teixeira-Clerc F., Julien B., Grenard P., Tran Van Nhieu J., Deveaux V., Li L., Serriere-Lanneau V., Ledent C., Mallat A. and Lotersztajn S. (2006). Cb1 cannabinoid receptor antagonism: A new strategy for the treatment of liver fibrosis. Nat. Med. 12, 671-676.

Yu T.S., Cheng Z.H., Li L.Q., Zhao R., Fan Y.Y., Du Y., Ma W.X. and Guan D.W. (2010). The cannabinoid receptor type 2 is time-dependently expressed during skeletal muscle wound healing in rats. Int. J. Legal Med. 124, 397-404.

Zechner R., Zimmermann R., Eichmann T.O., Kohlwein S.D., Haemmerle G., Lass A. and Madeo F. (2012). Fat signals--lipases and lipolysis in lipid metabolism and signaling. Cell Metab. 15, 279-291.

Zhang S.T., Zhao R., Ma W.X., Fan Y.Y., Guan W.Z., Wang J., Ren P., Zhong K., Yu T.S., Pi J.B. and Guan D.W. (2013). Nrf1 is time-dependently expressed and distributed in the distinct cell types after trauma to skeletal muscles in rats. Histol. Histopathol. 28, 725-735.

Accepted April 29, 2015